Attitude Determination – Advanced Sun Sensors for Pico-satellites

Yonatan Winetraub (a), San Bitan, Uval dd
Dr Anna B. Heller (b)
Handasaim School, Tel-Aviv University, Israel

Abstract
This paper presents the development of a novel model to determine the attitude of a small, cubic shape, satellite in space relatively to the sun's direction.

The improvements discussed here help Pico satellites to perform accurate attitude determination with no need for additional hardware.

The theoretical and the practical sides of this project are analyzed .

1. INTRODUCTION

1.1. Pico-Satellites

A normal sized satellite usually weighs more than 500kg, is a few meters long and cost more than 1million Euro to build and launch. However, the smaller satellites: Micro, Nano and Pico (Pico Satellites are about the size of an Hungarian Cube: 10X10X10cm and weight less then 1kg) are cheaper to construct and launch, and can do several specifics tasks even better than large satellites.

Because of their small size, all onboard components are energy thrifty, and their entire surface is used to collect energy from the sun through solar panels.

1.2. STMC's Pico-Satellites Project

STMC (Space Tech Meyerhoff Collage, see Figure 1.1) is a 1-year curse witch teaches space technology to high-school students. At the end of the year, the students, like ourselves are given the possibility to deep their studies by participating in one of STMC's projects.

The main goal of the STMC program is the design of two Pico-satellites to be launched into space in fly formation within a range from 10 to 100 meters. They may be launched independently or from a larger "mother" satellite by inducing small differences in the orbit's inclination an ellipticity.
The first Pico-Satellite (STMC1) will carry two compact cameras (VIS and IR) with the mission to monitor the large satellite operation.
The second Pico-satellite (STMC2) will monitor the degradation of sample materials in the space environment by using a miniature spectrometer.

1.3. Attitude Determination (AD)

Attitude Determination is one of the most important subsystems on-board a satellite. This component determinates the satellite's orientation relatively to the Earth, Sun or other object. In our case it is important to know the orientation of STMC1 relatively to the large satellite so it can monitor it.
There are many ways to build a AD component; we will discuss some of them later on.

1.4. Sun Sensors

One of the most common AD systems are Sun Sensors, these sensors determine the satellite's orientation relatively to the sun by measuring the amount of light or shadow on them.
There are several types of Sun Sensors, however, in this article we will focus on Analog Sun Sensors because unlike other sensors, they use the onboard solar cells of the satellite without the need of additional hardware. At this project we will present a new technique for improving existing Analog Sun Sensors.

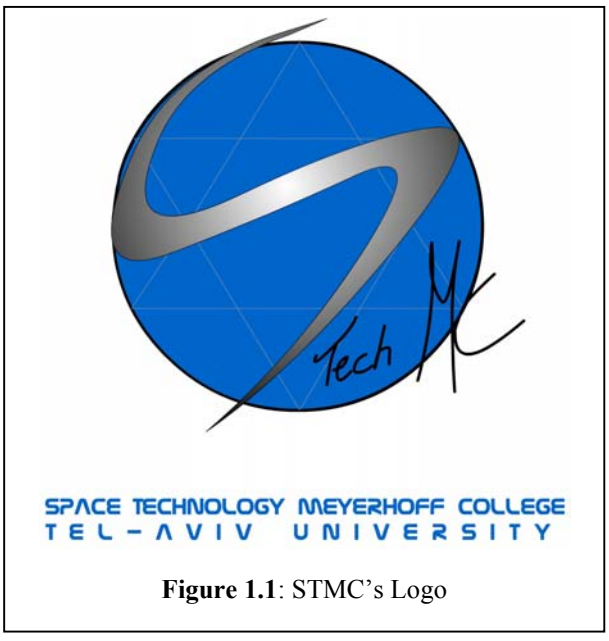

Figure 1.1: STMC's Logo

(a)Yonatan Winetraub, Head of STMC's System Engendering. Email: yokat@netvision.net.il.
(b) Dr Anna B. Heller, Head of STMC. Email: ana@wise.tau.ac.il.

2. THE EXISTING MARKET

2.1. Growing Number Of Smaller Satellites In Fly Formation

As of today, there is an increase in the number of Micro, Nano and Pico satellites, launched by many countries from Europe to the United States. These tiny satellites test some breakthrough technologies. This is mainly because the smaller price-to-pay in case of failure.

We will also see more satellites flying as a cluster. The reason for that is that a cluster of small satellites is chipper to construct and maintain and can perform more complex jobs than the single unit.

2.2. Existing Attitude Determination systems

These are several common AD systems found at the market; we will focus on the advantages and disadvantages of each component for a Pico Satellite.

- **Star Tracker** – This component images a part of the sky and by comparing a map of the sky to the picture, it can determine its orientation relatively to the stars. They have the higher accuracy of all AD systems but their size and weight are too large for Pico-satellites.
- **Horizon Scanner** – By measuring the relatively between the darkness of space and the light bouncing of the Earth, the Horizon Scanner finds the Earth's horizon thus the orientation relatively to the blue planet. Its problem is the low accuracy: about 1º accurate.
- **Magnetometer** – This sensor measures the intensity and direction of the Earth's magnetic field. This sensor has a medium accuracy of 1º, however its main disadvantage is that it can work only at LEO (Low Earth Orbits) because the magnetic field weaken with increasing altitude.
- **Gyro** – Like the Star tracker system, this component is too big to be inserted into a Pico-satellite.
- **Digital Sun Sensors –** These are one of the most accurate sun sensors available, the main problem is they need direct sunlight and so they are installed at the panels of the satellite instead of several solar cells. In our case that is critical problem because fewer solar cells means less power provided to the satellite.
- **Analog Sun Sensors –** As said before these are the most common used sensors, however, they are extremely inaccurate: 1º of accuracy in FOV (Field Of View) of 30º.

Because of the advantages of the Analog Sun Sensors for Pico-satellites we decided to try and improve them to a satisfactory accuracy level using an improved mathematical model called "J function".

3. HOW DOSE AN ANALOG SUN SENSOR WORKS?

In order to explain the improvements we did, we will start explaining how dose an analog sun sensor works. Analog sun sensors are composed of solar cells, therefore we will start with the question: how a solar cell works.

3.1. How A Solar Cell Works?

Solar cell is an electrical component based on a physical phenomenon called the "photo-electric effect".

This means that when a solar cell is exposed to light at a certain frequency it produces power. The amount of current depends on the light's frequency and brightness. The higher the frequency and the brighter the light is, the hire the power produced by the solar cell will be.

Because the sun's luminance and it's light are well known we can draw a function of the current and voltage produced by a single solar cell under various lightning conditions.

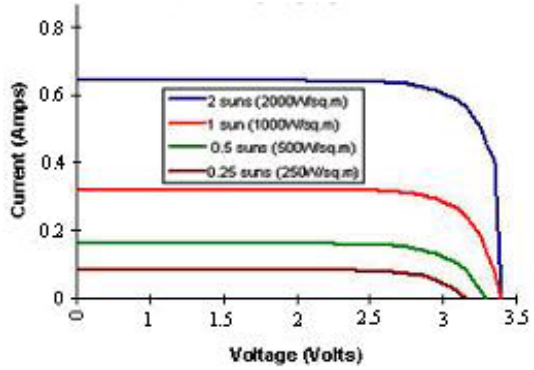

Figure 3.1: An example of current and voltage output of a single solar cell under varying lightning conditions. The solar cell, at its linear area (0 to 2.5 volts) acts like current supplier. At this figure we can

You can clearly see the behavior of a current supplier at the linear aria, and indeed you can see that in figure 3.2.

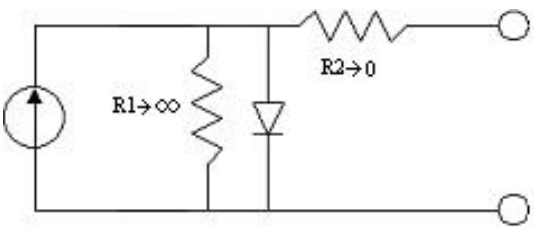

Figure 3.2: A solar cell electric model.

At this article, we will assume the solar cell is within the linear area.

3.2. How An Analog Sun Sensor Works?

As said before, the current (I) produced by a solar panel is directly connected to sunlight 's hit angle.
The function I (θ) that describe this phenomenon is been approximated to the sine function:

$$(1)\quad I(\theta) = I_{\max} \cdot \sin\theta$$

In 3 dimensions (3D):

$$(2)\quad \begin{aligned} I_{left} &= I_{\max} \sin\phi\cos\theta \\ I_{front} &= I_{\max} \cos\phi\cos\theta \\ I_{top} &= I_{\max} \sin\theta \end{aligned}$$

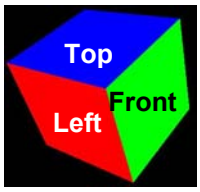

By measuring the current produced by 3 solar panels that share an apex, the sun vector (a single unit vector directing on the sun), can be calculated.
The sun vector in 3D is therefore defined by:

$$(3)\quad v_S^B = \begin{bmatrix} \sin\phi\cos\theta \\ \cos\phi\cos\theta \\ \sin\theta \end{bmatrix}$$

It can also be written using the intensity measurements:

$$(5)\quad v_S^B = \begin{bmatrix} X & 0 & 0 \\ 0 & Y & 0 \\ 0 & 0 & Z \end{bmatrix} \cdot \begin{bmatrix} I_{left} \\ I_{front} \\ I_{top} \end{bmatrix} \cdot \frac{1}{I_{\max}}$$

Where X, Y and Z equal 1 or –1 depending on the solar panel's location: on the positive or negative side of the satellite.

3.3. Why Analog Sun Sensors Are Inaccurate?

The main reason for the inaccuracy of these sensors is the sine model, as it can be seen in figure 3.3:

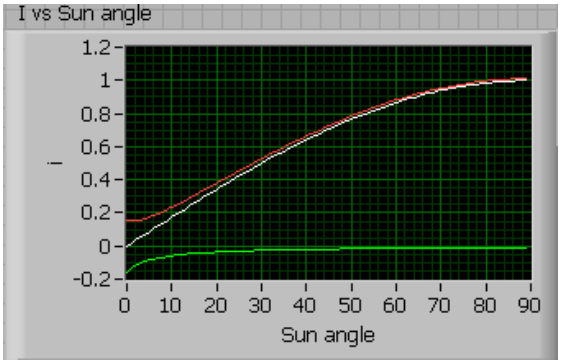

Figure 3.3: I vs. Sun Angle: in white - the sine model, in red - the measured I (θ) function, and in green – the difference

As can be seen, this approximation leads to wrong calculations when θ is close to 0º (when sunlight is almost parallel to the solar cell).
This happens mainly because of the apparent sun's diameter. When θ is close to 90º you cannot tell if the sun is a doted light source or a spherical light source and so the sine approximation works well.
On the contrary, when θ approaches 0º, half the sun has sunk below the solar cell and doesn't produce electrical current, and half the sun is shining on the solar panel producing current
(See figure 3.4).

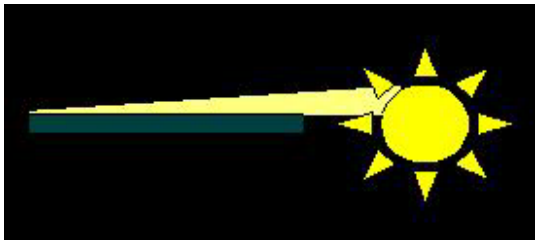

Figure 3.4: Half of the sun is still producing current though θ is close to 0º

As θ approaches 0º there is a large inaccuracy in the sine approximation as shown in figure 3.5.

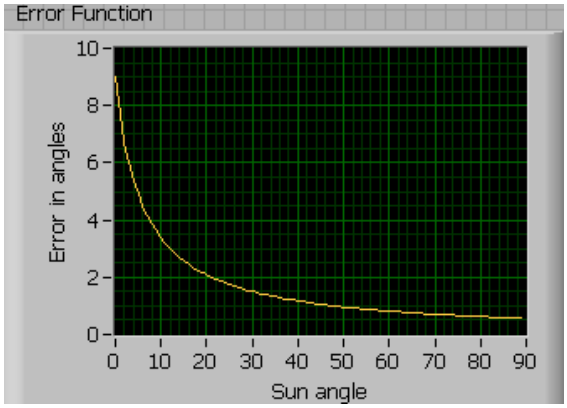

Figure 3.5: Accuracy (in degrees) relatively to sun angle. Accuracy drops as θ approaches 0º.

4. ADVANCED SUN SENSORS -MODEL

4.1. How Did We Improved The Accuracy

We decided to improve the existing mathematical model in order to gain greater accuracy.

To do so, we define the J function:

$$(6)\quad J(\theta) \equiv \frac{I_{\text{measured}}(\theta)}{I_{\max} \cdot \sin\theta}$$

Because of J's definition, it needs to be measured for each and every solar panel. (See Illustration for J function at figure 4.1). The more I measurements, the more accurate the J calculation will be.

As we will see in the next section, the AD component will have in its database the J functions of all the solar panels.

Using J, formula (1) turns into:

$$(7)\quad I = J(\theta) \cdot I_{\max} \cdot \sin\theta$$

Formula (5) turns into:

$$(8)\quad v_S^B = \begin{bmatrix} X & 0 & 0 \\ 0 & Y & 0 \\ 0 & 0 & Z \end{bmatrix} \cdot \begin{bmatrix} \frac{I_{left}}{J_1(\phi,\theta)} \\ \frac{I_{front}}{J_2(\phi,\theta)} \\ \frac{I_{top}}{J_3(\theta)} \end{bmatrix} \frac{1}{I_{\max}}$$

In order to extract the direction of the satellite from the current measurements of the solar panels we use formula (9) (for rotation in one axes only, a similar equation is derived for 2 axis rotation).

$$(9)\quad \theta = \arcsin\left(\frac{I_{\text{measured}}}{J(\theta_0) + \left.\frac{dJ}{d\theta}\right|_{\theta_0} \cdot \omega\Delta t} \cdot \frac{1}{I_{\max}} \right)$$

Where Θ is the estimated solar flux angle,
Θ_0 is the angle calculated at the last run, ω is the estimated angular speed and Δt is the time lap between two runs.

We assume that as long as the J function is well defined, Δt is small and the angular speed doesn't change much between two runs, a first degree approximation of a Taylor component will give a satisfactory accurate Θ. We will discuss more of this approximation later on.

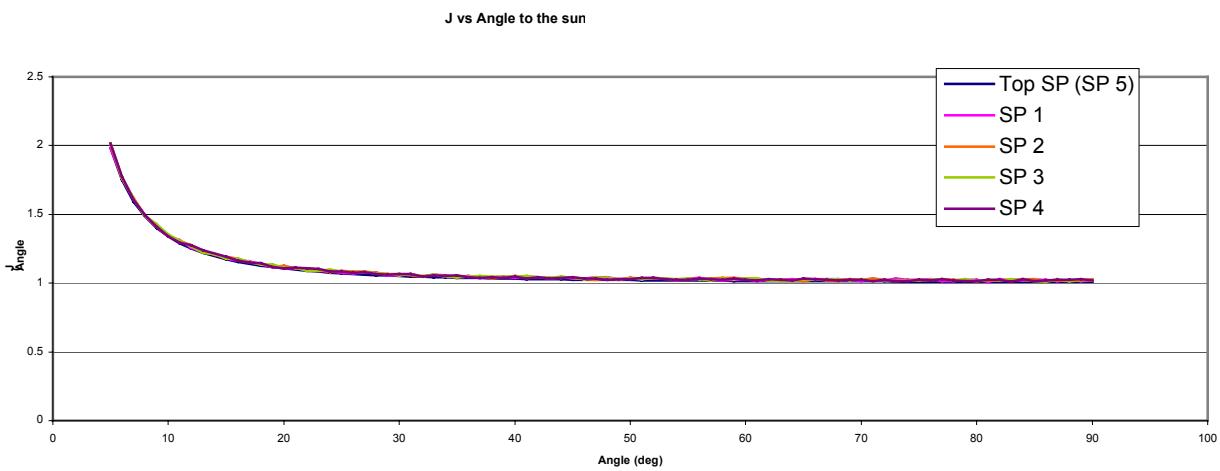

Figure 4.1: Illustration of several J functions derived from the same laboratory. All solar cells show a similar J functions with minor differences.

4.2. Shadow Problems

Because sun sensors deal with sunlight, we must take into consideration what will happen if sunlight is been blocked from the sensor and how to compensate on that lost.

There are three object that can shadow the Pico-satellites and thus three main problems:

1) The Earth – If the satellite is within "night zone".
2) The large satellite - As shown at figure 4.2, when the large satellite is close to the STMC's satellites it may cause shadow upon the solar panels.
3) The satellite itself – As only three sides of the cube can be illuminated by the sun and in our satellite one side of the six panels will not contain solar cells, it is clear that if sunlight hits that side, some orientation data will be lost.

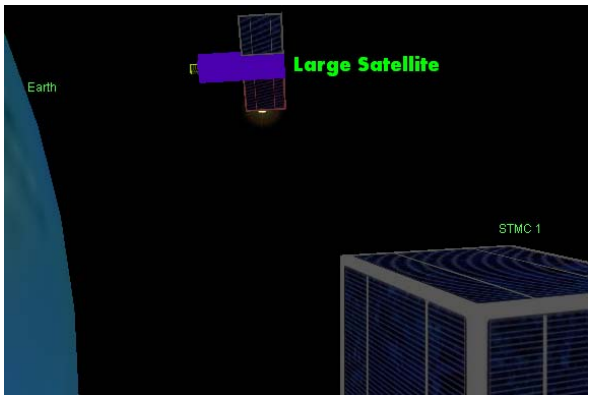

Figure 4.2: Illustration created by one of our simulation programs, you can see that The Large Satellite's solar panel is shadowing STMC 1 satellite.

The first two problems are solved by assuming that the angular velocity doesn't change much through nighttime. At that case, formula (9) still doses the trick. An additional AD sensor from the former mentioned can also solve that problem.

As for the third problem, we actually need only 2 solar panels in order to calculate the sun vector. The third solar panel is used to adjust the proper operation.
In case one measurement from a solar panel is missing, the algorithm will not tune its calculation and the satellite will sense a temporal drop in orientation's accuracy.

4.3. Dazzling Problems

In case of a short distances, the large satellite can dazzle the sun sensors in the picosats as shown in figure 4.3.
To deal with this problem, we built a mathematical filter.

Dazzling occur when sunlight bounces from a reflective surface such as a satellite's body or solar cells directly to the sun sensor. Notice that as sunlight bounces from a surface its luminance weakens due to the surface absorbing (see figure 4.4)

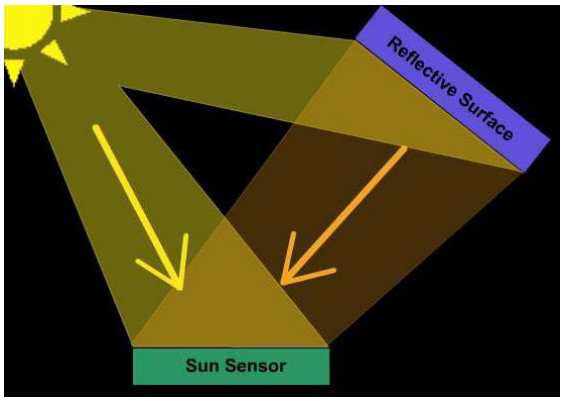

Figure 4.4: Both the sun and the reflective surface produces flux on the sun sensor, because of the surface's observation it reflects a smaller amount of light.

A B

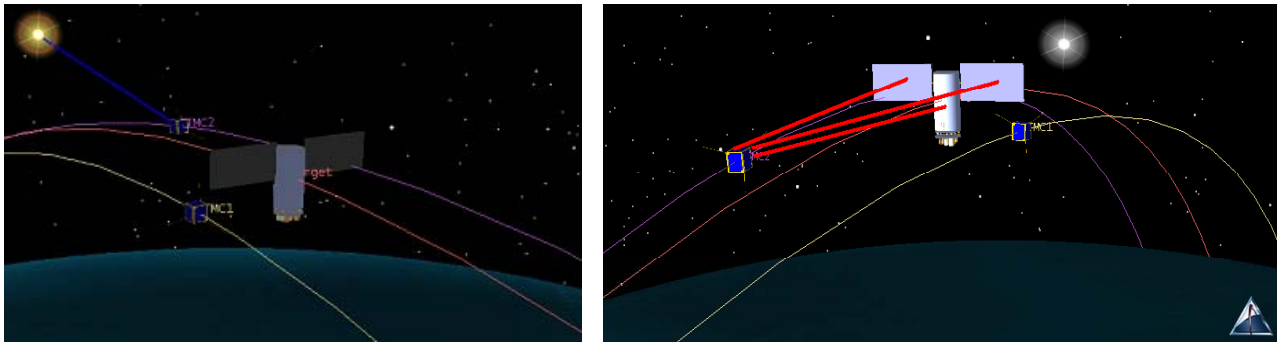

Figure 4.3: Illustration created by STK. Figures A and B describe the same scene from different looking angles. Because the large satellite is dazzling STMC 2, he might "think" there are 2 suns in the sky: the real one (at yellow), and a false sun in the opposite way shown in gray

The current produced by the light from the reflective surface is described in formula (10).

$$I = \alpha \cdot J(\theta_r) \cdot I_{\max} \cdot \sin\theta_r \quad (10)$$

Where α is the reflection coefficient (0<α<1); it describes how much of the incoming light is reflected back (α=0 – no light is reflected, α=1 all of the incoming light is reflected).
θr is the angle of witch the reflective light hits the sun sensor.

Our anti-dazzling filter substrates the current produced by the reflective light from the current measured to receive the current produced only by the direct sunlight (by the principle of superposition).

However, this is not always possible, a solar cell produces current relatively to the light flow as shown in figure 4.5. The principle of superposition will work only if the solar cell is within the linear area, in that case we will use formula 11 to determine orientation.
If the solar cell is within the saturation or warm-up area, we cannot use the principle of superposition and the dada from this solar cell will be lost.

$$I_{out} = I_{\text{measured}} - \alpha \cdot J(\theta_r) \cdot I_{\max} \cdot \sin\theta_r \quad (11)$$

Where I_{out} is the current exiting the filter, $I_{measured}$ is the current entering the filter.

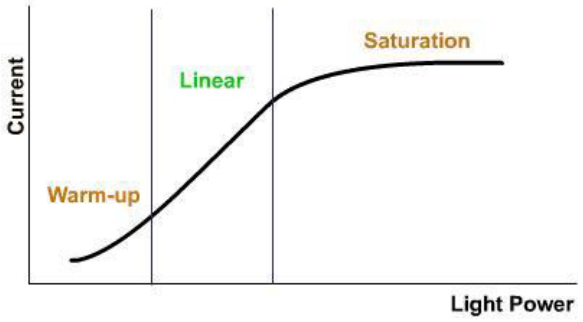

Figure 4.5: Current intensity changes as light power changes. The borders between the warm-up and linear, and linear and saturation areas differ from one solar cell to another.

5. ADVANCED SUN SENSORS –SOFTWARE DESIGN

In figure 5.1 you can see the flow chart of the proposed Advanced Sun Sensor.

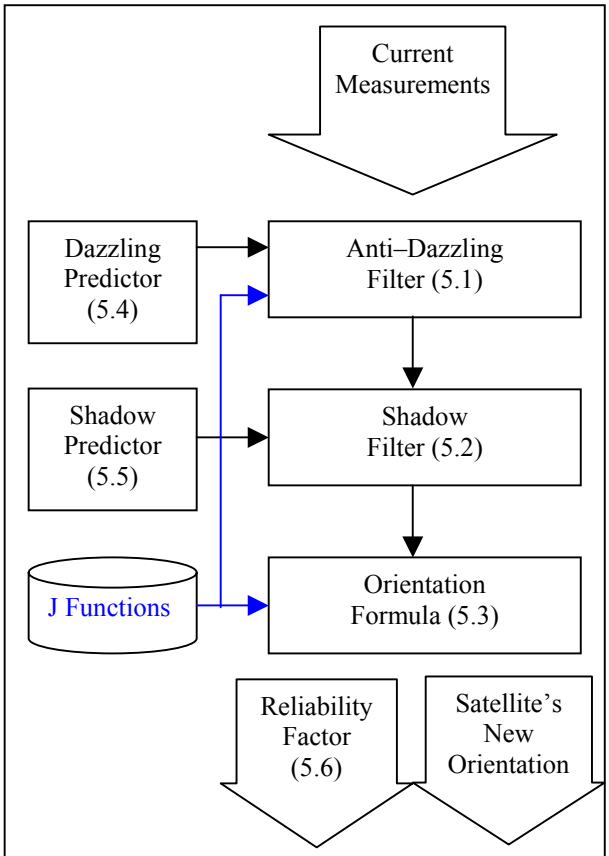

Figure 5.1: As new current measurements are included in the data, the Advanced Sun Sensor makes the calculations before the new orientation is determined

5.1. Anti–Dazzling Filter

This block implement formula (11) and filters all the dazzling effects. It receives the "θr" parameter from the "Dazzling predictor" component.

5.2. Shadow Filter

This component marks the solar cells that are been shadowed and ignores the data they produced.

5.3. Orientation Formula

This block calculates the actual sun vector by using formulas (8) and (9) and additional standard averaging.

5.4. Dazzling Predictor

This component predicts witch solar cells are been dazzled by using a 3-D model of the large satellite (see figure 5.2), and calculates the angle of witch the reflected light riches from (θr).

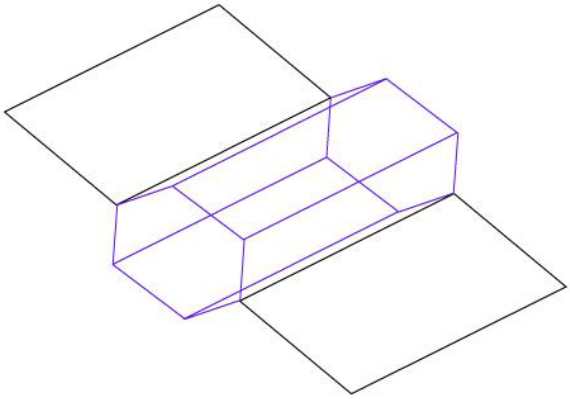

Figure 5.2: Ofeck 7 and Eros model, the body in purple is a hexagon; the solar panels in black are attached in the sides. Because the model is composed of flat square surfaces it is easy to calculate the optic reflections.

5.5. Shadow Predictor

Works on the same principle as the Dazzling Predictor.
However, this component calculates the solar cell that are been shadow.

5.6. Reliability Factor

As can be seen, the analog sun sensor has several levels of calculations: sometimes the sun sensor is been dazzled or shadowed and additional calculation is required (anti-dazzling filter etc).

The more calculations are required the less accurate the sun sensor will be.

This is why we defined the Reliability Factor, the higher the RF, the more trustable the sun sensor is.
RF scale drives from 1 to 10. 1-means the worst conditions: the satellite is within complete darkness. 10- means the sun is shining, no dazzling, no shadow.

6. COMPUTERIZED SIMULATIONS

6.1. Goals

The main goal of these simulations is to estimate what is the J function density required in order to gain 0.5 degrees accurate.

We also wanted to estimate what is the optimal sample rate ($\omega\Delta t$) that will allow this accuracy.

Another thing we check here is how fast does this algorithm reaches the required accuracy incase of mistake in previous measurements.

6.2. Tools

We used the following software:
- **STK** (Satellite Tool Kit) as a platform for the complex experiments.
- The algorithm was written using **LabView** and **C++**.
- We also used **MathLab** for data analysis.

6.3. Simulations

The first assumption we make is that there is a secondary AD system that takes over the Sun Sensor System over nighttime (when Earth blokes the sun).
We also assume that this secondary system has the accuracy of at least 10º and can produce a prediction of the angular speed witch is 10[deg/sec] accurate.

Simulation A: Using STK we fist tested different satellite orbits, and estimated what will be the average lightning conditions during daytime.

Simulation B: As a second stage, we estimated how accurate would be the angular speed 1 min after down breaks upon the satellite by using a single sun sensor. The variables here were J function accuracy and the sampling rate. We also used the average lighting conditions from the previous simulation.

Simulation C: At this simulation we estimated the average angular error produced by a single sun sensor rotating around 1 axis as we change the J function accuracy and the sampling rate. Here we used the average lightning conditions from Simulation A, and the average angular speed error from simulation B.
After this simulation we selected the optimal J function accuracy and the average sampling rate for our algorithm.

Simulation D: Finally we tested the algorithm by spontaneously noise it with series of false measurements and to see how fast it operate.

6.4. Results And Discussion

Simulation A: After testing several orbital conditions we roughly estimated the average lightning conditions as shown in figure 6.1. The reason it was hard to estimate these lightning conditions is because the final orbital parameters of our satellites are still uncertain due to several unresolved telemetry and picture broadcast related factors.

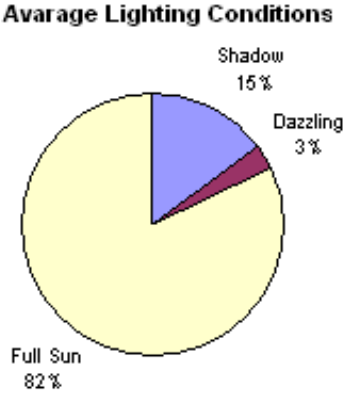

Figure 6.1: The breakdown of different lightning conditions over time by our estimation of "average lighting conditions". Notice that these conditions ignore the shadow cussed by the Earth.

Simulation B: When we tested this simulation over several angular speed and angle error we found that at most of the times the algorithm was able to reach a 10% accuracy within a reasonable time (2-7 sickles) as can be shown at figure 62. We must mention that there were several points in witch the algorithm wasn't able to reach the specified accuracy within the given time, this means that at simulation C we will give the algorithm at these points some better conditions to work at. However, as we will see, these points produce a large error even with this "help".

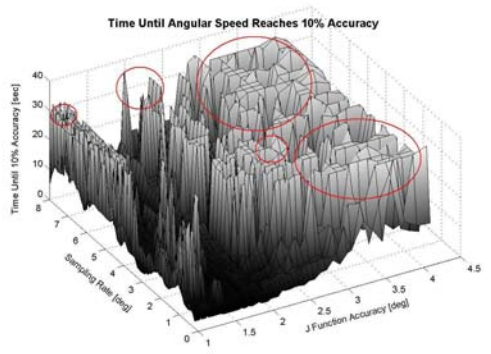

Figure 6.2: The average time until the algorithm calculates 10% accurate angular speed as sample rate and J function accuracy changes. The pikes circled in red are the points where the algorithm failed to produce this accuracy at the given time.

Simulation C: The results at figure 6.2 shows that there is a partial trade-off between J function accuracy and sampling rate, though the first one is more on the large scale.
We assume that if a single sun sensor can reach the average accuracy of 0.6º (shown as the red triangle at figure 6.3), a set of 3 sun sensors can reach the accuracy of 0.5º, this is why we choose the "target J function" to be 1º accurate, and average sample rate: $\omega\Delta t$=0.6º.

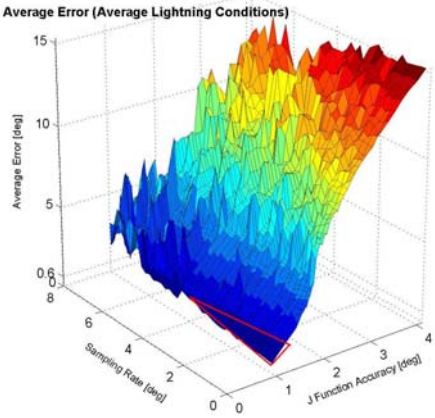

Figure 6.3: The average angular error provided by the sun sensor as sample rate and J function accuracy changes. The triangle in red marks the parameters that produce a satisfactory average error of 0.6º

Simulation D: As you can see in figure 6.4 the algorithm was able to overcome false measurements witch are 100º inaccurate (!). This is a remarkable finding, since we provided not only false measurements but also 3% background noise witch didn't seam to be a big problem for the algorithm.

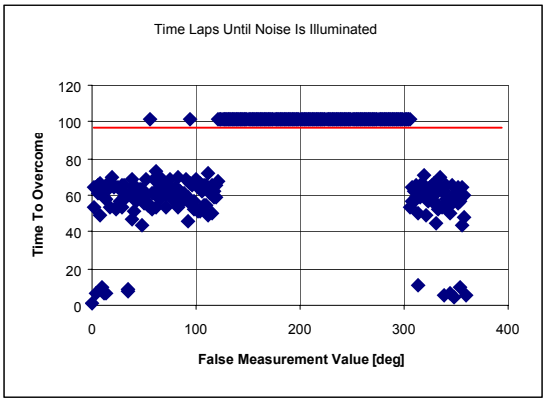

Figure 6.4: Time laps until the algorithm overcome on the false measurement. This time depends on the value of the false reading (X pivot).
The dots on the red line point out when the algorithm failed to provide suffusion accuracy within the given timeframe.

7. FIELD EXPERIMENT

7.1. Goal

At the field experiments we wanted to calculate a J function for a specific solar panel, then integrate it in our simulations for further analysis.

7.2. Tools

We used the following hardware:

- **Our testing module** shown in figure 7.1.
- **Data Logger** along with voltage-meter.

We also used the following software:

- A USA navy web site (1) that provided the suns altitude and azimuth.
- Data logger's software.

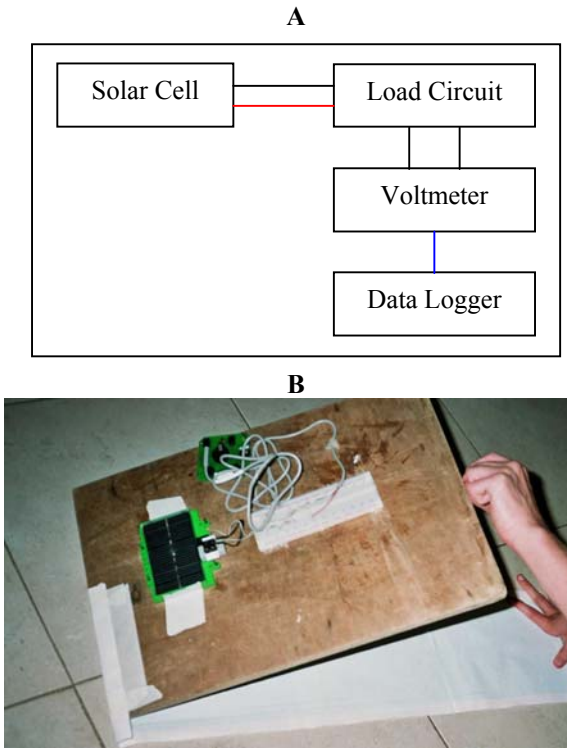

Figure 7.1: Our testing module, on figure A you can see the electrical design and on figure B a photograph of the testing module

7.3 Experiment

The experiment was conducted at midday at a sunny day because at noon the suns altitude changes slowly (about 0.4º over an hour) and there are very little clouds that can interrupt the testing.

We adjusted the solar panel to the sun direction in different attack angles and measured the current produced over these angles.

The angles where measured by the amount of shadow the testing module produces on the floor. This allows us to gain a J function witch is 1º accurate.

7.4 Results And Discussion

It can be can seen from the weather photo captured at the day of the experiment by our ground station (figure 7.2) it was indeed a sunny day.

Figure 7.2: NOAA 17's meteorological picture of Eastern Europe and Israel, captured by STMC's ground station at the day of the experiment, you can see there are very few clouds over Israel. Indeed it was a sunny day.

The "classical" graph of the measured current function relatively to the sine model is shown at figure 7.3.

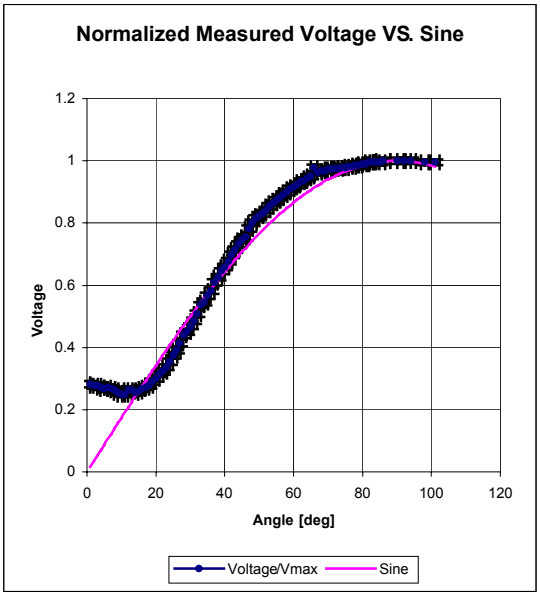

Figure 7.3: Normalized measured voltage vs. sine, you can clearly see the differences between the tow, spatially at small angles.

The normalized J function is shown at figure 7.4

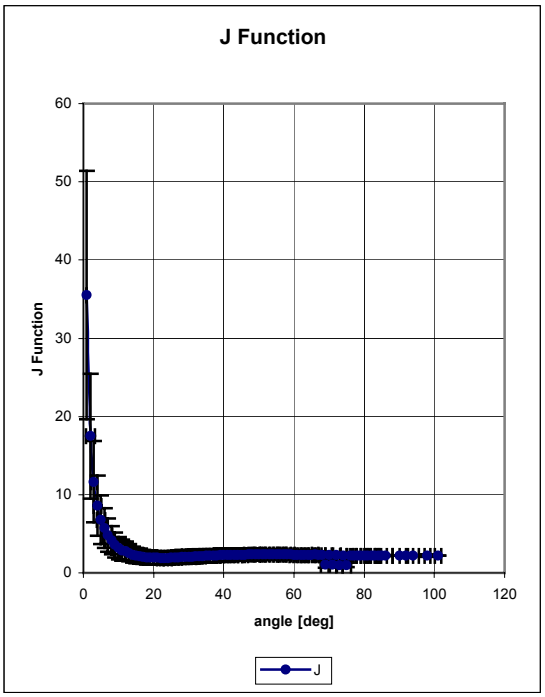

Figure 7.4: J function of the solar panel tested, you can see the similarities to the theoretical J function at the beginning of this article

8. CONCLUSIONS

Simulations and experiments show that a J function model as we presented here, can enhance sun sensors accuracy at least by factor of 2 (to 0.5 deg) and enhance the sensor's Field Of View (FOV) by factor of 2.5 (to 80 deg FOV).

These are remarkable findings for the Pico-Satellite market.

However, we must launch a Pico satellite carrying and testing this system. We estimate that such a launch may take place around 2007; therefore our final testing of the Advanced Sun Sensors will be over by 2008.

9. FUTURE WORKS

More simulations are needed at an advanced and complete stage in the design of STMC satellites.
The performance of our system may already be tested by Pico-Satellites currently operational by different universities around the world for full approval of the system performance.
Finally, launching STMC 1 and 2 into space with our Advanced Sun Sensors system on-board, will be the final implementation of the mission.

10. ACKNOWLEDGMENTS

We want to thank AGI (Analytical Graphics, Inc) and Synergy Integration LTD for providing us the STK analysis software tool kit. We are grateful to our friends from National Instruments for supporting us from the very beginning with training seminars and the LabView graphical development software.
We would also want to thank Naama Winetraub who helped us conduct the experiments.
And finally, to our ground station team at the Handasaim School, for the satellite meteorological pictures.

11. REFERENCES:

(1) http://aa.usno.navy.mil/data/docs/AltAz.html

(2) Attitude determination of the NCUBE satellite, 2003, Kristian Starveit.

(3) Attitude control for the Norwegian
Student satellite nCube, 2004, Eli Jerpseth O verby.

(4) Attitude Determination for AAU CubeSat, 2002, Kristian Krogh, Elmo Schreder and Thomas Bak.

(5) The Sun, 2004, Michael Stix.

(6) http://chuckwright.com/SolarSprintPV/
SolarSprintPV.html

(7)STMC
http://ths000.tau.ac.il/tautc/he/help_docs/stmc1/index.html